The Relationship Between Optic Disc and Retinal Artery Position and Glaucomatous Visual Field Progression

Yuri Fujino,[1,2] Ryo Asaoka,[1,3–6,] Hiroshi Murata,[4] and Takehiro Yamashita[7]

[1]Department of Ophthalmology, Seirei Hamamatsu General Hospital, Hamamatsu city, Shizuoka, Japan
[2]Department of Ophthalmology, Shimane University Faculty of Medicine, Matsue-shi, Shimane, Japan
[3]Seirei Christopher University, Hamamatsu city, Shizuoka, Japan
[4]Department of Ophthalmology, The University of Tokyo, Tokyo, Japan
[5]Nanovision Research Division, Research Institute of Electronics, Shizuoka University, Hamamatsu City, Shizuoka, Japan
[6]The Graduate School for the Creation of New Photonics Industries, Hamamatsu City, Shizuoka, Japan
[7]Department of Ophthalmology, Kagoshima University Graduate School of Medical and Dental Sciences, Sakuragaoka, Kagoshima, Japan

Correspondence: Ryo Asaoka, Department of Ophthalmology, University of Tokyo Graduate School of Medicine 7-3-1 Hongo, Bunkyo-ku, Tokyo 113-8655, Japan; rasaoka-tky@umin.ac.jp.

Received: January 30, 2021
Accepted: June 8, 2021
Published: September 9, 2021

Citation: Fujino Y, Asaoka R, Murata H, Yamashita T. The relationship between optic disc and retinal artery position and glaucomatous visual field progression. *Invest Ophthalmol Vis Sci.* 2021;62(12):6. https://doi.org/10.1167/iovs.62.12.6

Purpose. To investigate whether retinal structural parameters, including positions of the optic disc and major retinal arteries, affect glaucomatous progression of the visual field (VF).

Methods. In this cohort study, 116 eyes of 73 patients with primary open angle glaucoma (POAG) were included. VFs were measured using the Humphrey Field Analyzer 24-2 program and the VF was divided into seven sectors according to the corresponding optic disc angle. Average total deviation (TD) was calculated in each sector. Positions of major retinal arteries in the superotemporal and inferotemporal areas were decided by identifying the points where the retinal artery intersected the 3.4-mm-diameter circle around the optic disc. The relationship between sectorial TD VF progression rate and eight variables (age, mean and standard deviation of intraocular pressure during the observation period, baseline sectorial TD value, papillomacular bundle tilt angle, and axial length, along with superior/inferior arterial angle) was investigated.

Results. The main outcome measures were the association between retinal structural parameters and glaucomatous progression of VF. The superior retinal artery angular position was positively associated with sectorial TD progression rates in two central sectors in the inferior hemifield, which suggests faster VF progression where superior retinal artery angles are narrow. Papillomacular bundle tilt was not associated with TD progression rate in any sector.

Conclusions. Progression of the inferior VF was associated with the superior retinal artery angular position in this study of POAG.

Keywords: glaucoma, visual field, fundus photo

Glaucoma causes irreversible visual field (VF) damage[1] and is currently the second leading cause of blindness in the world.[2] Without doubt, the reduction of intraocular pressure (IOP) is useful to halt the worsening of VF damage,[3–7] however, other factors also influence VF progression. For instance, Sung et al.[8] and Han et al.[9] reported that glaucomatous VF progression is associated with differences in retinal structures, such as optic disc tilt and rotation. Detailed investigations of the importance of optic disc position, in relation to the macula, on glaucomatous VF damage[10] also support these results.

Structural measurements of the retina vary according to the elongation of an eye, which is itself related to myopia. We previously reported that the angle between the supratemporal and infratemporal peaks in the profile of the circumpapillary retinal nerve fiber layer RNFL (cpRNFL) narrows with the elongation of an eye,[11] and this is associated with alterations of the biomechanical properties of an eye.[12–14] Indeed, the cpRNFL peak angle can be accurately represented by the angle between supratemporal and infratemporal major retinal arteries (correlation coefficient equal to 0.92).[11] We also reported that correcting the cpRNFL thickness profile using the positions of the major retinal arteries significantly improved the structure-function association between cpRNFL thickness and VF sensitivity.[15] Of note, the magnitude of retinal stretch due to the elongation of an eye cannot be totally explained by axial length (AL), since there should be a wide variation of AL inherited at birth across individuals. For instance, if ALs of two eyes are identical in two different adults but were different at birth this must be explained by differing degrees of elongation that occurred during growth periods.[16] Supporting this, we have recently shown that the macular ganglion cell–inner plexiform layer (GCIPL) thickness becomes thin when the major retinal artery angle is narrow, even after adjustment for AL.[17]

The purpose of the current study was to investigate the importance of retinal parameters, including positions of the optic disc and major retinal arteries, on VF progression in POAG patients. As results are expected to differ across VF sectors (according to the corresponding location of the optic disc), analyses were conducted by dividing the VF into small sectors using a previously reported mapping between the VF and optic disc.[18]

Materials and Methods

This study was approved by the Research Ethics Committee of the Graduate School of Medicine and Faculty of Medicine at the University of Tokyo. Written informed consent was given by participants for their information to be stored in the hospital database and used for research. This study was performed in accordance with the tenets of the Declaration of Helsinki.

Subjects

This retrospective study included 116 eyes of 73 patients with primary open-angle glaucoma (POAG). All patients underwent eight reliable Humphrey Field Analyzer (HFA; Carl Zeiss Meditec AG, Dublin, CA, USA) 24-2 or 30-2 tests (SITA-standard program). All the patients underwent VF examination at least once, prior to the initiation of the follow-up series. Only the initial eight VFs of a patient were analyzed when a patient had more than eight VF test results. POAG was diagnosed as follows: 1) glaucomatous optic neuropathy was defined according to the recommendations of the Japan Glaucoma Society Guidelines for Glaucoma:[19] signs of glaucomatous changes were judged comprehensively, such as focal rim notching or generalized rim thinning, large cup-to-disc ratio with cup excavation with/without laminar dot sign, and retinal nerve fiber layer defects with edges at the optic nerve head margin; 2) presence of glaucomatous VF defects in at least one eye, defined as three or more contiguous total deviation (TD) points at $P < 0.05$, two or more contiguous points at $P < 0.01$, or a 10 dB difference across the nasal horizontal midline at two or more adjacent points, or mean deviation (MD) worse than −5 dB;[20, 21] and 3) no signs of angle closure. Eyes that experienced any surgical procedure, including trabeculectomy and cataract surgery, during the VF series period were excluded. Patients who previously underwent ocular surgery (except for successful cataract extraction) and have other ocular diseases that could affect VF sensitivity, such as diabetes mellitus retinopathy, corneal opacity, and macular diseases, were excluded.

VF Data

VF testing was performed using the HFA 24-2 or 30-2 test. Following the manufacturer's recommendation, fixed loss (FL) rate < 20% and false positive (FP) rate < 15% were defined as reliable data, and data that did not meet these were excluded. When VFs were obtained with the 30-2 test pattern, only the 52 test locations overlapping with the 24-2 test pattern were used in the analyses. The mean of the total deviation (TD) of the 52 test points in the HFA 24-2 test pattern was calculated (mTD). In addition, the VF was divided into seven areas (each corresponded to 30 degree optic disc sectors similarly to our previous reports,[15] but started from the horizontal line[22]), based on the mapping in a previous study.[18] (Fig. 1) Sectors in the temporal VF region were not analyzed. The mean of TD values was calculated for each sector. VF progression rates were calculated by extrapolating these mTD or sectorial mean TD values against time, similar to the MD trend analysis employed in the HFA.

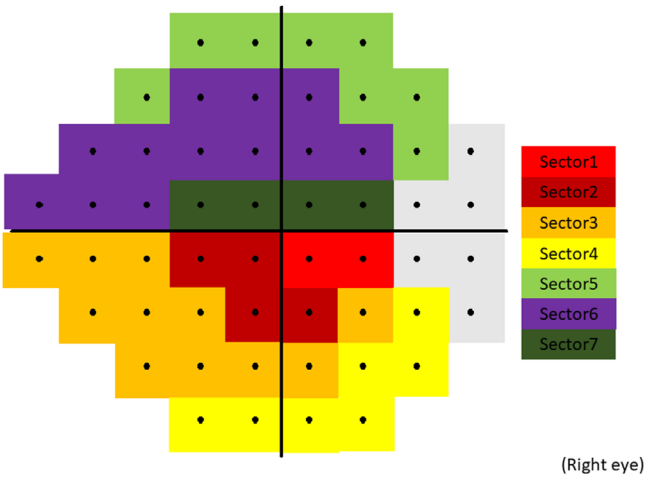

Figure 1. Visual field sectors. The visual field was divided into seven sectors, and the mean of the total deviation values for each sector was calculated progress from years.

Fundus Data

All fundus photographs were obtained with the 3D OCT-2000 (Topcon Corp., Tokyo, Japan) fundus camera during the VF observation period. All fundus image measurements were performed after pupil dilation by using a combination of tropicamide 0.5% with phenylephrine 0.5% (Mydrin-P; Santen, Osaka, Japan).

The rotation of the arterial angle and macular papilla position was calculated using ImageJ (version 1.52a, http://imagej.nih.gov/ij/; provided in the public domain by the National Institutes of Health, Bethesda, MD, USA) software in the same way as in our previous study.[15] In brief, first, the angle of the papillomacular bundle tilt was measured as the angle between the macula on the fundus photograph and the center of optic disc. Subsequently, the positions of major retinal arteries in the superotemporal and inferotemporal areas were automatically decided by identifying the points where the retinal artery intersects the 3.4-mm-diameter circle around the optic disc centered on the disc barycenter; the optic disc center was determined in fundus photographs as the barycenter of the closed spline curve fitted to the automatically determined seven points (with manual correction if required). The superior- and inferior- arterial angles were calculated as the angles against the papillomacular bundle tilt. (Fig. 2) The magnification effect was corrected according to the manufacturer-provided formula (a modified Littmann's equation),[20,21] which is based on measured refractive error, corneal radius, and axial length. Images influenced by involuntary blinking or saccade or those with a quality factor < 60% were excluded.

IOP Data

At least 11 (28.0 ± 8.91 [11 to 60], mean ± standard deviation: SD [range]) IOP measurements were conducted using

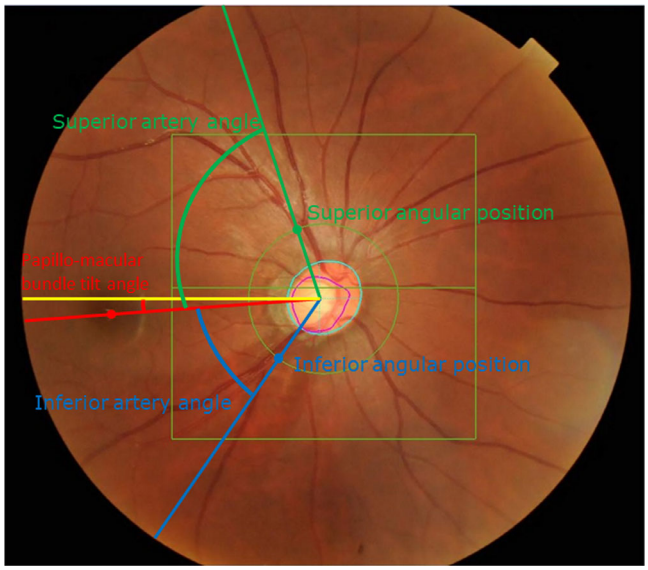

Figure 2. Measurement of arterial angle and papillomacular bundle tilt. The positions of major retinal arteries in the superotemporal and inferotemporal areas were automatically decided by identifying the points where the retinal artery intersects the 3.4-mm-diameter circle around the optic disc (*green and blue circles*, respectively), and the superior- and inferior-arterial angles were calculated as the angles against the papillomacular bundle tilt.

the Goldmann applanation tonometry during the observation period of VF test, and the mean and SD of IOP values during the observation period were calculated.

Other Measurements

AL was measured in all patients using the IOL Master, ver. 5.02 (Carl Zeiss Meditec AG).

Statistical Analysis

The association between mTD progression rate and eight variables were examined using the linear mixed model. The eight variables included five nonretinal parameters (age, mean IOP, SD of IOP during the observation period, baseline mTD value, and AL) and three retinal parameters (superior arterial angle, inferior arterial angle, and papillomacular bundle tilt angle). The linear mixed model is equivalent to ordinary linear regression in that the model describes the relationship between the predictor variables and a single outcome variable; however, standard linear regression analysis assumes that all observations are independent of each other, in contrast to the linear mixed model. In the current study, measurements were nested within subjects, and hence, dependent of each other. Ignoring this grouping of the measurements will result in the underestimation of standard errors of regression coefficients. The linear mixed model adjusts for the hierarchical structure of the data, modeling in a way in which measurements are grouped within subjects to reduce the possible bias derived from the nested structure of data.[23, 24] Subsequently, the optimal model was selected using the model selection method with the Akaike information criterion (AIC). The AIC is a well-established statistical measure used in model selection, and the AICc (Akaike information criterion with small-sample correction) is its corrected type, providing an accurate estimation especially when the sample size is small. [25] Variables in the optimal model (where AICc was minimized) were regarded as statistically significant.[26] Thereafter, similar optimal models were selected using sectorial mean TD progression rates. The variables included in the optimal models were considered significant. These analyses were iterated after scaling each variable, for the ease of understanding the effect of the variables.

All statistical analyses were performed using the statistical programming language R (ver. 3.6.1, The R Foundation for Statistical Computing, Vienna, Austria).

Table 1. Participant Characteristics

Participant Characteristics	Value
Age, years old at first VF (mean ± SD) [range]	58.3 ± 11.8 [29 to 85]
Gender (male/female)	79/37
Eyes (right/left)	56/60
AL, mm (mean ± SD) [range]	25.4 ± 1.73 [21.9 to 29.2]
Baseline mTD (dB) [range]	–4.3 ± 5.7 [–30.7 to –2.0]
Progression rate of mTD (dB) [range]	–0.23 ± 0.39 [–2.0 0.66]
Mean IOP (mmHg) [range]	13.9 ± 2.75 [6.8 to 23.3]
SD of IOP (mmHg) [range]	1.8 ± 0.58 [0.71 to 4.2]
Superior retinal artery angle (degree) [range]	63.5 ± 18.7 [15.9 to 99.2]
Inferior retinal artery angle (degree) [range]	59.6 ± 14.1 [12.5 to 97.2]
Papillomacular bundle tilt (degree) [range]	8.64 ± 3.9 [4.57 to 19.9]

SD: standard deviation, AL: axial length, mTD: mean of total deviation values, IOP: intraocular pressure.

Results

Characteristics of the study population are summarized in Table 1. The mTD value was –4.3 ± 5.6 dB (mean ± SD) and patient age was 58.3 ± 11.8 years at baseline. The progression rate of mTD was –0.23 ± 0.69 dB/year (Fig. 3). Superior and inferior retinal artery angle was 63.5 ± 18.7 and 59.7 ± 14.1 degrees, respectively.

Univariate analysis suggested that only age was significantly associated with mTD progression rate (coefficient = –0.0084, $P = 0.013$, linear mixed model), however other variables of mean IOP, SD of IOP during the observation period, baseline mTD value, and AL, along with superior arterial angle, inferior arterial angle, and papillomacular bundle tilt angle were not ($P > 0.05$); see Table 2. In the sector-wise analysis, age was significantly associated with sectorial VF progression rate in sectors 1, 3, and 4, but other variables were not significantly associated with the progression rate ($P > 0.05$, after the adjustment for multiple comparisons using the method proposed by Benjamini and Hochberg[27]).

The only variable selected in the optimal model for mTD progression rate (whole field) was age, with a coefficient value of –0.0084 (standard error (SE): 0.0032); see Table 3.

The variables included in the optimal models for the seven VF sectors were as follows (Table 3):

1) Sector 1: age (coefficient: −0.015, SE: 0.0054)
   baseline MD (coefficient: 0.029, SE: 0.018)
   superior artery angular position (coefficient: 0.0065, SE: 0.0033).

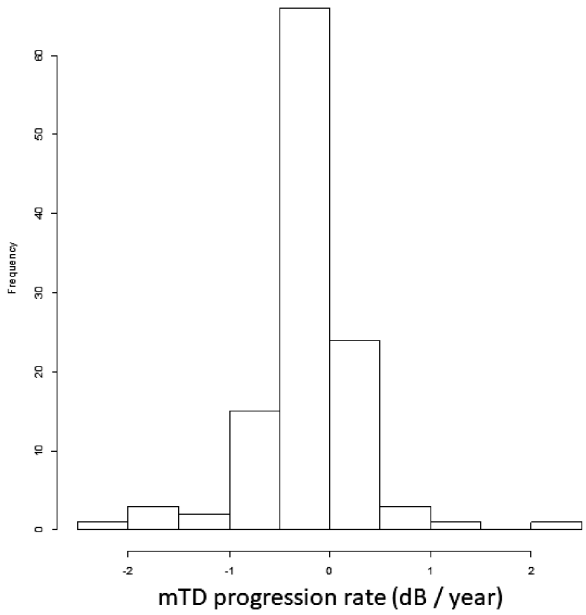

Figure 3. Histogram of the mTD progression rate. The progression rate of mTD was −0.23 ± 0.39 dB/year. mTD: mean of total deviation values.

2) Sector 2: age (coefficient: −0.020, SE: 0.0056) superior artery angular position (coefficient: 0.0075, SE: 0.0034)
3) Sector 3: age (coefficient: −0.011, SE: 0.0053) mean IOP (coefficient: −0.055, SE: 0.024)
4) Sector 4: age (coefficient: −0.0011, SE: 0.0043) baseline mTD (coefficient: 0.015, SE: 0.0082)
5) Sector 5: mean IOP (coefficient: −0.050, SE: 0.032) inferior artery angular position (coefficient: −0.0097, SE: 0.0050)
6) Sector 6: no variables selected
7) Sector 7: age (coefficient: −0.010, SE: 0.0060) SD of IOP (coefficient: −0.17, SE: 0.12)

Superior retinal artery angular position was positively associated with sectorial mTD progression rates in sectors 1 and 2, which suggests faster VF progression with a narrower superior retinal artery angle. Inferior retinal artery angular position was negatively associated with the sectorial mTD progression rate in sector 5. Papillomacular bundle tilt was not selected as an important predictor in any sector.

Table 4 shows these results after normalization:

1) Sector 1: age (coefficient: −0.18, SE: 0.064) baseline MD (coefficient: 0.093, SE: 0.060) superior artery angular position (coefficient: 0.12, SE: 0.064).
2) Sector 2: age (coefficient: −0.24, SE: 0.067) superior artery angular position (coefficient: 0.14, SE: 0.065)
3) Sector 3: age (coefficient: −0.14, SE: 0.063) mean IOP (coefficient: −0.15, SE: 0.066)
4) Sector 4: age (coefficient: −0.14, SE: 0.052) baseline mTD (coefficient: 0.097, SE: 0.052)
5) Sector 5: mean IOP (coefficient: −0.14, SE: 0.087) inferior artery angular position (coefficient: −0.14, SE: 0.071)
6) Sector 6: no variables selected
7) Sector 7: age (coefficient: −0.12, SE: 0.071) SD of IOP (coefficient: −0.10, SE: 0.069)

Table 2. Univariate Analysis Results

	Whole Field	Sector 1	Sector 2	Sector 3	Sector 4	Sector 5	Sector 6	Sector 7
Age								
Coefficient	**–0.0084**	–0.011	**–0.016**	–0.011	**–0.012**	–0.010	–0.0090	0.0036
P value	**0.035**	0.072	**0.031**	0.075	**0.035**	0.16	0.16	0.71
Mean IOP								
Coefficient	–0.0083	–0.096	–0.021	–0.053	–0.0060	–0.051	–0.028	0.024
P value	0.76	0.76	0.76	0.27	0.76	0.48	0.76	0.76
SD of IOP								
Coefficient	–0.011	0.015	0.021	0.0094	–0.073	–0.0082	–0.14	–0.052
P value	0.95	0.95	0.95	0.95	0.95	0.95	0.95	0.95
Baseline mTD								
Coefficient	0.0056	0.027	0.0062	0.0018	0.016	–0.0035	–0.0033	0.0022
P value	0.61	0.61	0.85	0.85	0.56	0.85	0.85	0.85
AL								
Coefficient	0.028	–0.12	0.023	0.052	0.0039	0.027	0.045	–0.052
P value	0.79	0.83	0.79	0.79	0.90	0.79	0.79	0.79
Superior artery angle								
Coefficient	0.00016	0.0037	0.0040	–0.00023	–0.0016	–0.0053	–0.0020	0.0035
P value	0.94	0.69	0.69	0.94	0.77	0.69	0.77	0.77
Inferior artery angle								
Coefficient	0.00080	0.0013	0.0051	0.0071	0.0035	–0.0098	0.0023	0.0063
P value	0.77	0.77	0.67	0.34	0.67	0.34	0.77	0.67
Papillomacular bundle tilt angle								
Coefficient	0.0014	–0.0096	–0.0014	–0.0032	0.00053	–0.0020	–0.00096	–0.0041
P value	0.97	0.97	0.97	0.97	0.97	0.97	0.97	0.97

IOP: intraocular pressure, SD: standard deviation, AL: axial length, mTD: mean of total deviation values.

Table 3. Linear Mixed Model Results (Original Scale)

	Whole Field	Sector 1	Sector 2	Sector 3	Sector 4	Sector 5	Sector 6	Sector 7
Age								
Coefficient	−0.0084	−0.015	−0.020	−0.011	−0.0011	N.S.	N.S.	−0.010
Standard Error	0.013	0.0054	0.0056	0.0053	0.0043			0.0060
Mean IOP								
Coefficient	N.S.	N.S.	N.S.	−0.055	N.S.	−0.050	N.S.	N.S.
Standard Error				0.024		0.032		
SD of IOP								
Coefficient	N.S.	N.S.	N.S.	N.S.	N.S.	N.S.	N.S.	−0.17
Standard Error								0.12
Baseline mTD								
Coefficient	N.S.	0.029	N.S.	N.S.	0.015	N.S.	N.S.	N.S.
Standard Error		0.018			0.0082			
AL								
Coefficient	N.S.	N.S.	N.S.	N.S.	N.S.	N.S.	N.S.	N.S.
Standard Error								
Superior artery angular position								
Coefficient	N.S.	0.0065	0.0075	N.S.	N.S.			
Standard Error		0.0033	0.0034					
Inferior artery angular position								
Coefficient	N.S.					−0.0097	N.S.	N.S.
Standard Error						0.0050		
Papillo-macular bundle tilt angle								
Coefficient	N.S.	N.S.	N.S.	N.S.	N.S.	N.S.	N.S.	N.S.
Standard Error								

IOP: intraocular pressure, SD: standard deviation, AL: axial length, mTD: mean of total deviation values, N.S.: not selected.

Discussion

We investigated the relationship between VF progression and age, AL, superior and inferior artery angular positions, papillomacular bundle tilt angle, mean IOP, SD of IOP, and baseline sectorial mTD. We observed that a narrow superior arterial angle was associated with faster VF progression in two sectors (sectors 1 and 2) and a wider inferior artery angular position was associated with more rapid VF progression in one sector (sector 5). Papillomacular bundle tilt angle was not associated with VF progression rate in any sector.

In the current study, the mean mTD progression rate was –0.23 dB/year with a mean baseline mTD value of –4.3 dB. These values were very similar to that in our previous study (–0.26 dB/year and an mTD of –6.9 dB) in which VF data was collected from 710 eyes in 490 patients with open-angle glaucoma at multiple real-world clinics (University Hospitals) in Japan.[28] On the other hand, this mTD progression rate is considerably slower than those reported in other studies from real-world clinics. For instance, De Moraes et al. reported an average –0.45 dB/year VF progression rate with a mean baseline MD value of –7.1 dB in 587 patients with glaucoma.[29] Heijl et al. reported an average VF progression rate of –0.80 dB/year with a median baseline MD value of –10.0 dB in 583 patients with open-angle glaucoma.[30] These differences could be attributed to the difference of the IOP control during the observation period (15.2 mmHg[29] or between 18.1 and 20.5 mmHg[30] compared to 13.9 mmHg in the current study).

Table 4. Linear Mixed Model Results (After Normalization)

	Whole Field	Sector 1	Sector 2	Sector 3	Sector 4	Sector 5	Sector 6	Sector 7
Age								
Coefficient	−0.10	−0.18	−0.24	−0.14	−0.14	N.S.	N.S.	−0.12
Standard Error	0.039	0.064	0.067	0.063	0.052			0.071
Mean IOP								
Coefficient	N.S.	N.S.	N.S.	−0.15	N.S.	−0.14	N.S.	N.S.
Standard Error				0.066		0.087		
SD of IOP								
Coefficient	N.S.	N.S.	N.S.	N.S.	N.S.	N.S.	N.S.	−0.10
Standard Error								0.069
Baseline mTD								
Coefficient	N.S.	0.093	N.S.	N.S.	0.097	N.S.	N.S.	N.S.
Standard Error		0.060			0.052			
AL								
Coefficient	N.S.	N.S.	N.S.	N.S.	N.S.	N.S.	N.S.	N.S.
Standard Error								
Superior artery angular position								
Coefficient	N.S.	0.12	0.14	N.S.	N.S.			
Standard Error		0.064	0.065					
Inferior artery angular position								
Coefficient	N.S.					−0.14	N.S.	N.S.
Standard Error						0.071		
Papillo-macular bundle tilt angle								
Coefficient	N.S.	N.S.	N.S.	N.S.	N.S.	N.S.	N.S.	N.S.
Standard Error								

IOP: intraocular pressure, SD: standard deviation, AL: axial length, mTD: mean of total deviation values, N.S.: not selected.

Previous studies have hypothesized the importance of papillomacular bundle tilt on glaucomatous VF damage. For instance, Abe et al. suggested a less negative disc-fovea angle was associated with more advanced central visual field damage.[31] This was also observed in a separate study.[32] However, an epidemiological study in Japan showed no difference in the papillomacular bundle tilt angle between normative and glaucomatous eyes.[33] Finding similar results, papillomacular bundle tilt angle was not associated with VF progression rate in any sector in the current study. A possible reason may be that this angle between the disc-fovea axis and the horizontal axis in the image plane, is subject to cyclotorsion, that is, the rotation of the head. If the head is differently rotated when the same eye is repeatedly measured, the rotation angle can be different, which would introduce additional noise. On the other hand, a narrow superior arterial angle was associated with VF progression in two sectors (sectors 1 and 2). We recently reported that the retina is stretched, and the macular GCIPL becomes thin, when the major retinal artery angle is narrow, even after adjustment for AL.[17] The reason for this association and the importance on the progression of glaucoma is still to be elucidated, however, as we now observe a narrow superior retinal artery angle may be associated with faster VF progression in VF sectors 1 and 2. In contrast, the opposite tendency was observed between the position of the inferior retinal

artery and VF progression rate in sector 5. The result appears contradictory, but we postulate that this area of the VF is affected by the superior eye lid and an accurate assessment of VF damage is difficult. In addition, retinal area originally located in more central area is shifted toward the periphery in eyes with a wider superior artery angle. Sector 6 corresponds to the Bjerrum scotoma, and this sector is one of the most preferentially affected VF areas in glaucoma. As a result, sector 5 tends to include more retina originally corresponding to sector 6 when the AL angle is large. This may be another reason why inferior artery angular position was inversely correlated with the progression of VF in sector 5.

Sectors 1 and 2 correspond to the optic disc 0 to 30 and 30 to 60 degrees below the papillomacular bundle, respectively;[18] these regions are generally resilient to glaucomatous change, as reported by Hood et al.[10] However, as shown in our previous paper, the retina is shifted toward the papillomacular bundle in eyes with a narrow artery angle. Indeed, we previously reported that adjusting the cpRNFL using the artery position strengthened the structure-function relationship.[15] Consequently, in eyes with a narrow artery angle, we would expect retinal nerve fibers from a more vulnerable area (the inferotemporal area) would be included in these measurements.[34] Indeed, it has been shown that retinal nerve fiber layer defects tend to locate closer to the fovea in glaucomatous eyes with the retinal artery closer to the fovea.[35] Also, it was suggested that this inferior central area is mostly spared whenever glaucoma patients develop central vision loss, regardless of the rest of the visual field or the general vision loss severity.[36] This may be another reason for observing faster VF progression (in sectors 1 and 2) in eyes with a narrow superior artery angle. Of note, the results with the normalization suggest the effect of the narrowing of the superior artery angle (coefficients = 0.12/0.14) was not negligible at least compared to other variables, such as age (coefficients = –0.18 or –0.24), baseline mTD (0.093) and mean IOP (coefficients = –0.15 or –0.14). In particular, mean IOP was a significant parameter in sector 5 corresponds to the superior vulnerability zone identified by Hood et al.[10]

Many papers have considered myopia as a risk factor for the onset [37–39] and progression [8, 40, 41] of glaucoma. In myopic eyes, the optic disc is deformed according to the elongation of the eye.[42] The magnitude of myopia is usually assessed using AL, however, we previously reported that the magnitude of retinal stretch (due to the elongation of an eye) cannot be explained by AL alone; a more accurate approximation can be achieved using the retinal artery position.[11] In the current study, AL was not associated with the VF progression rate in any sector, in contrast to retinal artery angular positions. This suggests that a detailed analysis of retinal stretch using the retinal artery position, not merely AL, might better reveal the effect of retinal stretch on the progression of glaucoma. Previously, we suggested that AL changes, even in adults.[43] The difference in AL was merely 0.035 mm in five years but, nonetheless, it was significantly associated with the progression of glaucoma. This implies the position of retinal arteries can also vary over time, and this should be investigated in a future study. Of note, we did not conduct any analyses in long eyes separately. This was because it is not appropriate to segment using the AL value.[11] For instance, if ALs of two eyes were different at birth but the same in adulthood, then the degree of elongation must have differed between these eyes during a growth period.[16]

Wang et al. have investigated the relationship between the positions of major retinal vessels and glaucoma severity in the cross-sectional manner.[44] As a result, it was suggested that peripapillary superior artery positions are significantly nasalized in advanced glaucoma, which agrees with the current results in sectors 1 and 2. It should be noted that this finding was observed when artery position was identified at 1.23 mm and 1.73 mm radius around the optic disc center, however, no effects were found for higher eccentricities, where this value was 1.73 mm in the current study. Wang et al. also reported substantial association between more nasal locations of the central retinal vessel trunk (CRVT: the location within the optic nerve head where all retinal blood vessels enter the eye from the brain) and more severe central vision loss in glaucoma, but not at any other locations of the VF.[45] This effect may translate to major blood vessels in the circumpapillary area, and if this is the case, all retinal blood vessels get "dragged into nasal direction".

The current study suggests limited influence of mean IOP on the progression rate of VF (it was only an important variable to explain progression in sectors 3 and 5). Very similar results were observed in our previous study using a multicentral VF data in Japan (JAMDIG study).[28] This result does not deny the effectiveness of IOP reduction on the progression of glaucoma as confirmed in many previous studies,[3–7] because all of the included patients were under treatment at glaucoma clinic. Indeed, these two sectors correspond to the superior and inferior poles of the optic nerve head, which corresponds to the superior vulnerability zone.[10] Also, albeit the relatively large magnitude of coefficient values (Table 4), the importance of this parameter cannot be underestimated. Nonetheless, the current results suggest the importance of other variables (retinal features) on the progression of glaucoma. Indeed, the Collaborative Normal-Tension Glaucoma Study showed that approximately 20% of patients continued to progress despite very successful IOP-treatment results (30 % reduction of IOP).[4] The current results might be useful when considering the mechanism of progression of glaucoma in these cases.

A limitation of our study is that VF assessment was conducted using the HFA 24-2 test. Sectors 1 and 2 mainly locate within the field of the HFA 10-2 test pattern, and hence, it would be beneficial to conduct an equivalent study using the HFA 10-2 test. In addition, analyses were not conducted in the temporal VF areas because of the small number of test points in the HFA 24-2 test.

In conclusion, the progression of the inferior VF was associated with the superior retinal artery angular position.

Acknowledgments

Supported by Grants 20768254, 25861618 and 19H01114, 18KK0253, and 26462679 from the Ministry of Education, Culture, Sports, Science, and Technology of Japan, the Translational Research program. Grants from the Strategic Promotion for practical application of Innovative medical Technology (TR-SPRINT) from the Japan Agency for Medical Research and Development (AMED), and grant AIP acceleration research from the Japan Science and Technology Agency.

Disclosure: **Y. Fujino,** None; **R. Asaoka,** None; **H. Murata,** None; **T. Yamashita,** None

References

1. Aoki S, Murata H, Fujino Y, et al. Investigating the usefulness of a cluster-based trend analysis to detect visual field progression in patients with open-angle glaucoma. *Br J Ophthalmol*. 2017;101(12):1658–1665.

2. Quigley HA, Broman AT. The number of people with glaucoma worldwide in 2010 and 2020. *Br J Ophthalmol*. 2006;90(3):262–267.
3. Garway-Heath DF, Crabb DP, Bunce C, et al. Latanoprost for open-angle glaucoma (UKGTS): a randomised, multicentre, placebo-controlled trial. *Lancet*. 2015;385(9975):1295–1304.
4. The effectiveness of intraocular pressure reduction in the treatment of normal-tension glaucoma. Collaborative Normal-Tension Glaucoma Study Group. *Am J Ophthalmol*. 1998;126(4):498–505.
5. Heijl A, Leske MC, Bengtsson B, et al. Reduction of intraocular pressure and glaucoma progression: results from the Early Manifest Glaucoma Trial. *Arch Ophthalmol*. 2002;120(10):1268–1279.
6. Kass MA, Heuer DK, Higginbotham EJ, et al. The Ocular Hypertension Treatment Study: a randomized trial determines that topical ocular hypotensive medication delays or prevents the onset of primary open-angle glaucoma. *Arch Ophthalmol*. 2002;120(6):701–713; discussion 829–30.
7. Ederer F, Gaasterland DE, Sullivan EK, Investigators A. The Advanced Glaucoma Intervention Study (AGIS): 1. Study design and methods and baseline characteristics of study patients. *Control Clin Trials*. 1994;15(4):299–325.
8. Sung MS, Kang YS, Heo H, Park SW. Optic disc rotation as a clue for predicting visual field progression in myopic normal-tension laucoma. *Ophthalmology*. 2016;123(7):1484–1493.
9. Han JC, Lee EJ, Kim SH, Kee C. Visual field progression pattern associated with optic disc tilt morphology in myopic open-angle glaucoma. *Am J Ophthalmol*. 2016;169:33–45.
10. Hood DC, Raza AS, de Moraes CG, et al. Glaucomatous damage of the macula. *Prog Retin Eye Res*. 2013;32:1–21.
11. Yamashita T, Asaoka R, Tanaka M, et al. Relationship between position of peak retinal nerve fiber layer thickness and retinal arteries on sectoral retinal nerve fiber layer thickness. *Invest Ophthalmol Vis Sci*. 2013;54(8):5481–5488.
12. Matsuura M, Murata H, Nakakura S, et al. The relationship between retinal nerve fibre layer thickness profiles and CorvisST tonometry measured biomechanical properties in young healthy subjects. *Sci Rep*. 2017;7(1):414.
13. Asano S, Asaoka R, Yamashita T, et al. Visualizing the dynamic change of ocular response analyzer waveform using variational autoencoder in association with the peripapillary retinal arteries angle. *Sci Rep*. 2020;10(1):6592.
14. Asano S, Asaoka R, Yamashita T, et al. Correlation between the myopic retinal deformation and corneal biomechanical characteristics measured with the Corvis ST tonometry. *Transl Vis Sci Technol*. 2019;8(4):26.
15. Fujino Y, Yamashita T, Murata H, Asaoka R. Adjusting circumpapillary retinal nerve fiber layer profile using retinal artery position improves the structure-function relationship in glaucoma. *Invest Ophthalmol Vis Sci*. 2016;57(7):3152–3158.
16. Axer-Siegel R, Herscovici Z, Davidson S, et al. Early structural status of the eyes of healthy term neonates conceived by in vitro fertilization or conceived naturally. *Invest Ophthalmol Vis Sci*. 2007;48(12):5454–5458.
17. Omoto T, Murata H, Fujino Y, et al. Relationship between macular ganglion cell thickness and ocular elongation as measured by axial length and retinal artery position. *Invest Ophthalmol Vis Sci*. 2020;61(11):16.
18. Garway-Heath DF, Poinoosawmy D, Fitzke FW, Hitchings RA. Mapping the visual field to the optic disc in normal tension glaucoma eyes. *Ophthalmology*. 2000;107(10):1809–1815.
19. Japan Glaucoma Society, https://ryokunaisho.jp/english/index.html.
20. Anderson DR, Patella VM. *Automated Static Perimetry*. 2nd ed. St. Louis: Mosby; 1999.
21. Hodapp E, Parrish RK, II, DR A. *Clinical Decisions in Glaucoma*. St Louis: The CV Mosby Co.; 1993.
22. Asaoka R, Russell RA, Malik R, et al. A novel distribution of visual field test points to improve the correlation between structure-function measurements. *Invest Ophthalmol Vis Sci*. 2012;53(13):8396–8404.
23. Baayen RH, Davidson DJ, Bates DM. Mixed-effects modeling with crossed random effects for subjects and items. *J Mem Lang*. 2008;59(4):390–412, https://www.sciencedirect.com/science/article/abs/pii/S0749596X07001398.
24. Bates D, Mächler M, Bolker B, Walker S. Fitting linear mixed-effects models using lme4. *J Stat Softw*. 2015;67(1).
25. Burnham KP, Anderson DR. Multimodel inference: understanding AIC and BIC in model selection. *Sociol Methods Res*. 2004;33(2):261–304.
26. Johnson DH. The insignificance of statistical significance testing. *J Wildl Manage*. 1999;63:763–772.
27. Benjamini Y, Hochberg Y. Controlling the false discovery rate: a practical and powerful approach to multiple testing. *J Royal Stat Soc Ser B*. 1995;57:289–300.
28. Fujino Y, Asaoka R, Murata H, et al. Evaluation of glaucoma progression in large-scale clinical data: the Japanese archive of multicentral databases in glaucoma (JAMDIG). *Invest Ophthalmol Vis Sci*. 2016;57(4):2012–2020.
29. De Moraes CG, Juthani VJ, Liebmann JM, et al. Risk factors for visual field progression in treated glaucoma. *Arch Ophthalmol*. 2011;129(5):562–568.
30. Heijl A, Buchholz P, Norrgren G, Bengtsson B. Rates of visual field progression in clinical glaucoma care. *Acta Ophthalmol*. 2013;91(5):406–412.
31. Abe RY, Matos AG, Gracitelli CPB, et al. Disc-fovea angle is associated with visual field defect location in patients with glaucoma. *J Glaucoma*. 2020;29(10):964–969.
32. Park HL, Kim YC, Jung Y, Park CK. Vertical disc tilt and features of the optic nerve head anatomy are related to visual field defect in myopic eyes. *Sci Rep*. 2019;9(1):3485.
33. Mataki N, Tomidokoro A, Araie M, Iwase A. Morphology of the optic disc in the Tajimi Study population. *Jpn J Ophthalmol*. 2017;61(6):441–447.
34. Yamashita T, Sakamoto T, Yoshihara N, et al. Correlations between retinal nerve fiber layer thickness and axial length, peripapillary retinal tilt, optic disc size, and retinal artery position in healthy eyes. *J Glaucoma*. 2017;26(1):34–40.
35. Yamashita T, Nitta K, Sonoda S, et al. Relationship between location of retinal nerve fiber layer defect and curvature of retinal artery trajectory in eyes with normal tension glaucoma. *Invest Ophthalmol Vis Sci*. 2015;56(10):6190–6195.
36. Wang M, Shen LQ, Pasquale LR, et al. Artificial intelligence classification of central visual field patterns in glaucoma. *Ophthalmology*. 2020;127(6):731–738.
37. Xu L, Wang Y, Wang S, et al. High myopia and glaucoma susceptibility the Beijing Eye Study. *Ophthalmology*. 2007;114(2):216–220.
38. Mastropasqua L, Lobefalo L, Mancini A, et al. Prevalence of myopia in open angle glaucoma. *Eur J Ophthalmol*. 1992;2(1):33–35.
39. Marcus MW, de Vries MM, Junoy Montolio FG, Jansonius NM. Myopia as a risk factor for open-angle glaucoma: a systematic review and meta-analysis. *Ophthalmology*. 2011;118(10):1989–94.e2.
40. Chihara E, Liu X, Dong J, et al. Severe myopia as a risk factor for progressive visual field loss in primary open-angle glaucoma. *Ophthalmologica*. 1997;211(2):66–71.
41. Lee YA, Shih YF, Lin LL, et al. Association between high myopia and progression of visual field loss in primary

Investigative Ophthalmology & Visual Science

open-angle glaucoma. *J Formos Med Assoc*. 2008;107(12): 952–957.

42. Samarawickrama C, Mitchell P, Tong L, et al. Myopia-related optic disc and retinal changes in adolescent children from Singapore. *Ophthalmology*. 2011;118(10):2050–2057.
43. Yanagisawa M, Yamashita T, Matsuura M, et al. Changes in axial length and progression of visual field damage in glaucoma. *Invest Ophthalmol Vis Sci*. 2018;59(1):407–417.
44. Wang M, Jin Q, Wang H, et al. Quantifying positional variation of retinal blood vessels in glaucoma. *PLoS One*. 2018;13(3):e0193555.
45. Wang M, Wang H, Pasquale LR, et al. Relationship between central retinal vessel trunk location and visual field loss in glaucoma. *Am J Ophthalmol*. 2017;176:53–60.

Investigative Ophthalmology & Visual Science